AD-772 677

ELECTRON BEAM MICROANALYSIS OF ELECTRO-CHEMICAL ATTACK ON THIN FILM NICKEL-CHROMIUM RESISTORS

John J. Bart

Rome Air Development Center
Griffiss Air Force Base, New York

October 1973

DISTRIBUTED BY:

NTIS

National Technical Information Service
U. S. DEPARTMENT OF COMMERCE
5285 Port Royal Road, Springfield Va. 22151

BEST AVAILABLE COPY

UNCLASSIFIED

SECURITY CLASSIFICATION OF THIS PAGE (When Data Entered)

AD-772677

REPORT DOCUMENTATION PAGE		READ INSTRUCTIONS BEFORE COMPLETING FORM
1. REPORT NUMBER RADC-TR-73-220	2. GOVT ACCESSION NO.	3. RECIPIENT'S CATALOG NUMBER
4. TITLE (and Subtitle) ELECTRON BEAM MICROANALYSIS OF ELECTROCHEMICAL ATTACK ON THIN FILM NICKEL-CHROMIUM RESISTORS		5. TYPE OF REPORT & PERIOD COVERED In-House Report 6. PERFORMING ORG. REPORT NUMBER RADC-TR-73-220
7. AUTHOR(s) John J. Bart		8. CONTRACT OR GRANT NUMBER(s) N/A
9. PERFORMING ORGANIZATION NAME AND ADDRESS Rome Air Development Center (RBRP) Griffiss Air Force Base, New York 13441		10. PROGRAM ELEMENT, PROJECT, TASK AREA & WORK UNIT NUMBERS Job Order No. 55190639
11. CONTROLLING OFFICE NAME AND ADDRESS Same		12. REPORT DATE October 1973 13. NUMBER OF PAGES 32
14. MONITORING AGENCY NAME & ADDRESS(if different from Controlling Office) Same		15. SECURITY CLASS. (of this report) Unclassified 15a. DECLASSIFICATION/DOWNGRADING SCHEDULE N/A

16. DISTRIBUTION STATEMENT (of this Report)

Approved for public release; distribution of this document is unlimited

17. DISTRIBUTION STATEMENT (of the abstract entered in Block 20, if different from Report)

Same

18. SUPPLEMENTARY NOTES

None

19. KEY WORDS (Continue on reverse side if necessary and identify by block number)

Reliability
Integrated Circuits
Thin Film Resistors
Corrosion
Electron Beam Microanalysis

Reproduced by
NATIONAL TECHNICAL
INFORMATION SERVICE
U S Department of Commerce
Springfield VA 22151

20. ABSTRACT (Continue on reverse side if necessary and identify by block number)

The performance of recently developed integrated circuits was evaluated for several types of environmental and electrical stress conditions. The principal cause of failure in these devices was the electrochemical attack of the thin film nickel-chromium resistors evaporated on the surface of these circuits.

DD FORM 1 JAN 73 1473 EDITION OF 1 NOV 65 IS OBSOLETE

UNCLASSIFIED

SECURITY CLASSIFICATION OF THIS PAGE (When Data Entered)

PREFACE

In order to establish the problems inherent in the use of low-power radiation-hardened integrated circuits in high reliability Air Force electronic systems, a program of device test and analysis was undertaken at the Rome Air Development Center.

This report is an account of the various analyses which led to the description of the basic failure mode of these circuits -- the electrochemical attack of the thin film nickel-chromium resistors.

The success of this study was dependent on the contributions of many people. Among my co-workers at RADC, I would like to thank V. C. Kapfer, for the electrical testing of the circuits; R. W. Thomas, for the mass spectrometry evaluation of the device ambient gas; B. H. Hommel for the determination of the device hermetic seal quality; and J. S. Smith, R. Bellem, and C. Lane for their discussions and suggestions concerning the fabrication and application aspects of the test circuits.

Special thanks are given T. Ellis of the Naval Ammunition Depot at Crane, Indiana, for performing the scanning electron microscopy portion of this study.

This report has been reviewed by the RADC Information Office (OI) and is releasable to the National Technical Information Service (NTIS).

This technical report has been reviewed and is approved.

APPROVED: John J. Bart
JOHN J. BART
Reliability Physics Section
Reliability Branch

APPROVED: Joseph J. Naresky
JOSEPH J. NARESKY
Chief, Reliability & Compatibility Div.

FOR THE COMMANDER:
CARLO P. CROCETTI
Chief, Plans Office

SUMMARY

The performance of recently developed integrated circuits was evaluated for several types of environmental and electrical stress conditions. The principal cause of failure in these devices was the electrochemical attack of the thin film nickel-chromium resistors evaporated on the surface of these circuits.

An electron beam microanalyzer was used to chemically analyze the reacted resistor films. The x-ray spectrochemical data obtained with this instrument was used to identify the basic nature of the electrochemical reaction. Important structural defects in these devices were examined with a scanning electron microscope. Finally, mass spectrometry was used to characterize the gas found inside the hermetically-enclosed device package.

These analytical techniques identified the steps which led to the observed attack of the thin film Ni-Cr resistors.

(a) Moisture present inside the hermetic package, under low temperature operating conditions, would preferentially condense in defect sites in the deposited glass layer over the resistors.

(b) Sodium contamination, arising from the glass materials used to make the device package, ionized the condensed water and caused an excess hydroxyl ion concentration.

(c) The hydroxyl ions reacted with the thin film resistors resulting in the formation of complex anions of both nickel and chromium.

(d) Potentials applied to the device caused the negative complex ions to migrate to positively biased points on the surface of the device.

(e) The chemical attack and subsequent electrochemical transport of ions proceeded until the nickel and chromium was completely removed, thereby resulting in an open resistor.

Based on these findings, the following recommendations were made in order to minimize the susceptibility of this type of integrated circuit to failure:

(a) Use a defect-free deposited glass layer which is compatible with the temperature levels required to fabricate a packaged device.

(b) Eliminate contaminants such as water and sodium through proper process control procedures.

(c) Assure proper device hermetic seal integrity through the proper choice of package materials.

CONTENTS

LIST OF ILLUSTRATIONS

LIST OF TABLES

I. INTRODUCTION

The use of nickel-chromium alloys for precision electrical resistors is not a novel application of these materials. However, it has only been within the past several years that these compounds have been combined with silicon monolithic integrated circuit (IC) technology. By replacing the normal diffused resistor structures of these devices with a thin film of Ni-Cr, the new class of devices exhibited improved temperature stability, lower parasitic capacitance, and a better resistance to radiation.

A recent survey[1] of the use of such thin film structures in microelectronics discusses the various advantages of such a scheme in greater detail. It also describes the new technology's most serious drawback: the difficulty in achieving compatibility among the thin film materials, the types of processing; and other materials employed in making a finished integrated circuit.

At RADC a program of device testing and analysis was undertaken to establish the effects of the structural and chemical factors present in these circuits on the behavior of the thin film nickel-chromium resistors.

At the outset of the study, consideration was given to many different types of stresses which might affect thin film resistor performance. This work and that of Philofsky[2] et al, established that the various metallurgical reactions which take place between the nickel-chromium material and the aluminum metallization stripes used to interconnect various parts of the active device were not a determining factor in the behavior of the thin film resistors. Instead, the electrochemical attack of these films under low temperature conditions was the principal cause of failure of the devices that were being studied.

The purpose of this report is to present the results of the electron beam microanalysis (EBM) studies which have led to the development of a model for the observed electrochemical reaction. The intent was to correlate, principally through use of an electron microprobe, the various chemical characteristics of the integrated circuit with the behavior of thin film nickel-chromium resistors. Other pertinent features of the devices were studied with several additional techniques including scanning electron microscopy and mass spectrometry, as will be shown in subsequent sections of this report.

Once the various observations were explained by a single comprehensive model, the final result was the development of recommendations for minimizing the susceptibility of integrated circuits to this mode of failure.

II MATERIALS AND METHODS

A. NICKEL-CHROMIUM TEST FILMS

Because of the basic interest in studying the behavior of thin film nickel-chromium resistors on actual monolithic integrated circuit structures, the test devices used for this study were commercially manufactured digital circuits. Figure 1 depicts the important physical features of the thin film resistor structures.

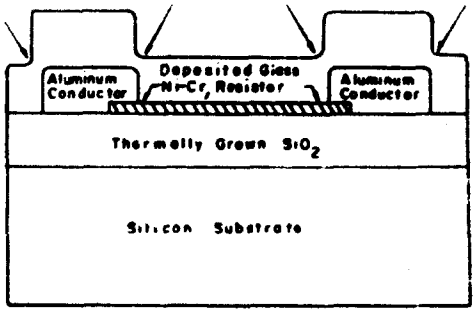

Figure 1. Ni-Cr Thin Film Test Structure

The Ni-Cr films were deposited, using filament evaporation techniques, to a thickness of approximately 150 Angstroms on a thermally oxidized silicon substrate. Interconnection of the resistor elements with the various diffused areas of the IC was accomplished by the evaporation and delineation of an aluminum metallization layer of 9000 Angstroms thickness. A 1 micrometer thick protective "glassivation" layer was then vacuum deposited over both films. This glass layer, comprised of undoped SiO_2, was supposed to serve two functions: (1) to prevent mechanical damage to the thin film resistors during subsequent device processing, and (2) to inhibit chemical attack of these elements.

The reader's attention is directed to the regions near the edge of the aluminum stripe, as indicated by the arrows. As will be shown in a later section of this report, cracks in the glass layer at these points contribute significantly to the failure of the nickel-chromium resistors. Figure 2 is a photograph of a completed test circuit before final hermetic sealing of the package. The arrows indicate the location of the Ni-Cr resistors.

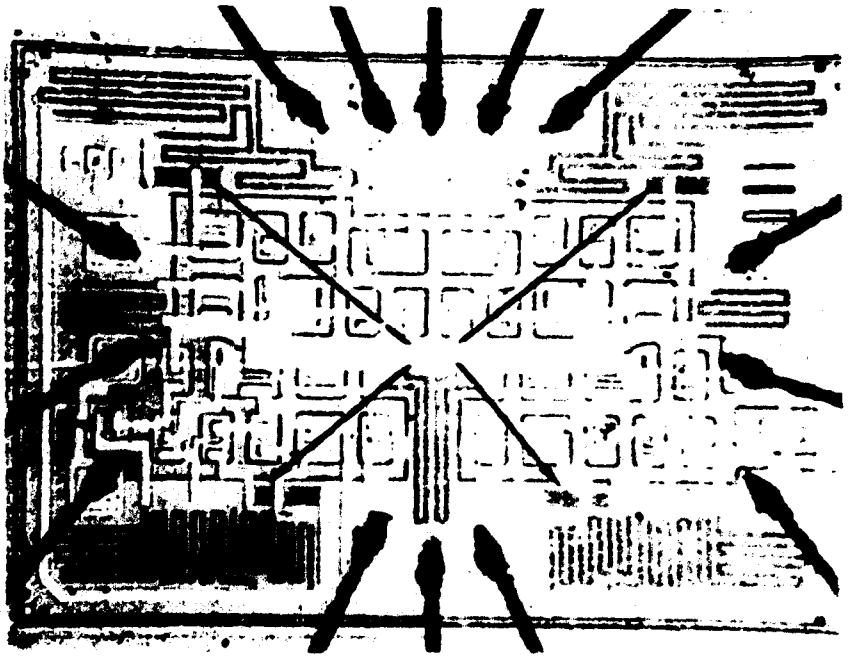

Figure 2. Completed Test Circuit

As will be shown later, the type of package used for these devices plays an important part in the electrochemical attack of the Ni-Cr films. Figure 3 is a cross-sectional diagram of the all-ceramic package used for the test devices. The aluminum bonding pad areas are exposed by chemically etching the deposited SiO_2 layer. The devices are then placed in the bottom part of the package. Electrical connection of the integrated circuit to the outside world is provided by ultrasonically bonded 1 mil aluminum wires extending between the bonding pads and the package lead frame.

A glass bond between both the metal and the ceramic materials secures the metal lead frame. After the aluminum wires are bonded, the lid of the package is sealed at high temperatures with a devitrifying solder glass-ceramic material. The intent of these processes is to provide a hermetically sealed environment for the integrated circuit.

B. TEST PROCEDURES

All of the device test conditions were chosen to accelerate or enhance the electrochemical attack of the thin Ni-Cr films. Standard electrical biasing circuitry assured the correct determination of the voltage and current conditions at each critical point on the test devices.

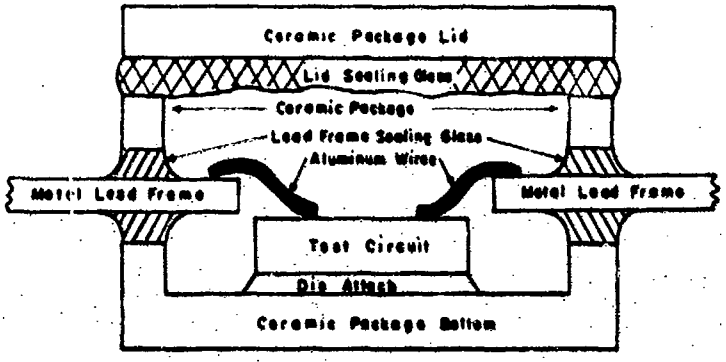

Figure 3. Ceramic Package Cross Section

In addition to standard environmental test chambers, a "Thermospot Cold Probe" was used to thermally cycle a biased test device for a rapid determination of the conditions causing thin film attack. The salient features of the "Thermospot" and other tests will be described in greater detail in Section III.

C. ANALYTICAL TECHNIQUES

1. The Electron Beam Microanalyzer

The principal approach to the study of the electrochemical attack of thin film Ni-Cr resistors has been through the use of an electron beam microanalyzer (EBM). This instrument, described in Castaing's thesis[3], combines the essential characteristics of both x-ray emission spectroscopy and electron microscopy. A detailed description of many aspects of this technique is beyond the scope of this report. However, interested readers are referred to an excellent treatise[4] by L. S. Birks. The most important features of an EBM are depicted schematically in Figure 4.

A beam of high energy electrons is focused on the surface of the sample by two magnetic lenses to a spot diameter of less than one square micron. The primary electron beam is of sufficient energy to generate, in addition to bremsstrahlung radiation, the characteristic x-ray spectra of the elements present in the sample. A complement of several curved crystal spectrometers is used to analyse dispersively the various x-ray wavelengths. These crystal spectrometers are designed with a constant "take-off" angle Φ, in order to facilitate the analytical treatment of the x-ray intensity data. A rotation of the curved and ground crystal through the angular range of θ then satisfies the Bragg diffraction condition:

$$n\lambda = 2d \sin\theta$$

for each value of λ.

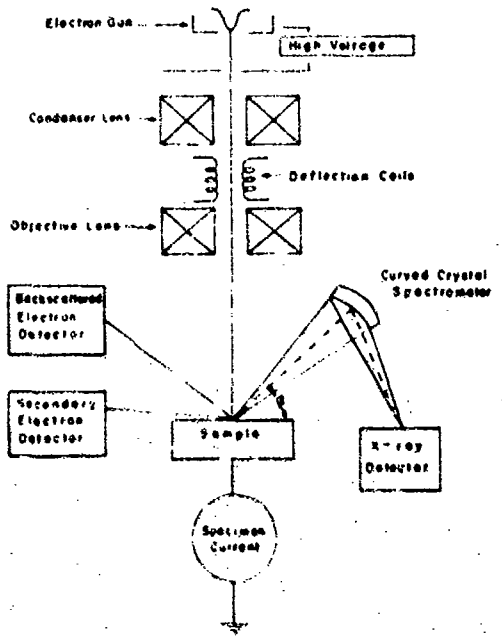

Figure 4. Electron Beam Microanalyzer Block Diagram

In addition to the principal function of x-ray spectrochemical analysis, most EBM's are also designed for detection and display of the following electron signals:

(a) Primary or high energy backscattered electrons;

(b) Absorbed primary electrons, referred to as specimen current;

(c) Secondary or low energy electrons emitted from the region bombarded by the primary beam.

The various outputs of the EBM are displayed in the following ways:

(a) Digital Output - The x-ray count rate is recorded using scaler counting circuitry.

(b) Analog Output - Either the x-ray signals, after suitable electronic integration, or the various electron signals are displayed on strip chart recorders.

(c) Scanning Displays - By synchronously scanning both the primary electron beam and a display oscilloscope in a raster pattern, the different EBM outputs are used to form x-ray or electron scanning micrographs.

The first two types of outputs are normally used for quantitative analysis in which intensity values are recorded for characteristic wavelengths of a given element from both a standard and an unknown. The third display mode, while providing only qualitative information, is the one most widely used in the analysis of electronic devices.

The output of an x-ray spectrometer is used to modulate the display oscilloscope, the resultant micrograph represents a pictorial "map" of the distribution of a given element near the surface of the scanned area of the sample. On the other hand, the scanning electron microscope is used to study the structural characteristics of the surface. The actual signal for this purpose is the secondary electron response since the resolution of this technique is comparable to the diameter of the electron beam, usually 0.1 μm. The range of electrons in the sample are the backscattered and absorbed electron signals.

The magnification of the scanning micrographs is determined by taking the ratio of the length of the line on a display scope to the length of the line on the surface of the sample. The standard range of magnification of such EBM scanning displays is between 10X and 10,000 X.

Electron beam microanalysis is ideally suited to the chemical characterization of the thin nickel-chromium films under study because of the excellent absolute detectability limits it provides for an element with an atomic number greater than five. The reason for these low limits is that the EBM will detect x-rays generated from within an excited volume of less than 10 cubic microns. The exact size of this volume depends on the energy of the primary beam and the material being examined. Typically, only 10^{-9} or 10^{-10} grams of material are being sampled under these conditions. The assumption that a particular element can be detected in a relative concentration of 100 ppm in this volume leads to a figure of 10^{-13} or 10^{-14} grams for the absolute detectability limit.

The true concentration of a given element is obtained by recording the intensity of the characteristic x-rays from both the unknown and a standard. By multiplying the observed intensity ratio by suitable correction factors (which account for the interaction of both the primary electrons and generated x-rays with the sample) elemental composition in terms of weight percent can be determined with an accuracy of ±10%. The nature of the various correction factors is discussed in considerable detail in two recent books.[4], [5]

The EBM used on this study is a commercially available instrument manufactured by Applied Research Laboratories, Inc. It has three Johansson curved crystal spectrometers. Each spectrometer has a 52.5 degree take-off angle. This high value of ϕ not only results in minimum spectrometer shadowing effects due to surface irregularities of the sample, but it also minimizes the absorption of the detected x-rays by having the spectrometer "look" at x-rays which have passed through a thinner layer of the sample, i.e., the x-ray path length. The amount of absorption is therefore proportional to cosecant ϕ. This design feature of the EBM is especially important in the detection of long wavelength K-series x-rays emitted by the low atomic number elements.

Two of the spectrometers use sealed proportional counters in conjunction with either a lithium fluoride (LiF) or ammonium dihydrogen phosphate (ADP) crystal. These two crystals are used for the analysis of elements greater in atomic number than 12. The third spectrometer, equipped with an ultra-thin window flow proportional counter and either a lead stearate decanoate (PbSD) or rubidium acid phthalate (RAP) crystal, is used for light element analysis, i.e., $5<Z<13$.

The important parameters established at the outset of the EBM analyses included:

(a) A Determination of Electron Range: A high energy beam of electrons will generate x-rays from a volume of material determined by the electron energy. The particular values of electron range vs. accelerating potential were estimated for the materials present in our test structures. The estimate was reached by using a method proposed by Archard and Mulvey[6] and electron range coefficients tabulated by Nelms[7]. The calculated values, shown in Table I, enabled the proper choice of accelerating potential essential in studying the layered structures found on the test devices.

TABLE I

ELECTRON RANGE CALCULATION AS A
FUNCTION OF ACCELERATING POTENTIAL

	RANGE (μm)				
Material	10 KV	15 KV	20 KV	25 KV	30 KV
Aluminum	1.32	2.62	4.35	6.38	8.81
Silicon	1.42	2.89	4.75	7.00	9.60
Chromium	0.60	1.18	1.92	2.83	3.85
Nickel	0.49	0.95	1.56	2.24	3.12
Silicon Dioxide	1.34	2.75	4.52	6.66	9.24

(b) Choice of Characteristic X-Ray Lines: After initial qualitative determination of the important elements involved in the electrochemical attack of Ni-Cr films, the various characteristic lines shown in Table II were chosen for the subsequent analyses. This work was done to establish the required critical energy for the emission of the various x-rays and to enable the selection of the proper crystal for each wavelength, also shown in this table.

TABLE II

X-RAY LINES AND ANALYZING CRYSTALS

EMITTER	$\lambda K_{\alpha 1,2}$ (ANGSTROMS)	$E_{CRIT\ K\alpha\ 1,2}$ (KEV)	CRYSTAL
Oxygen	23.707	0.532	Rubidium Acid Phthalate
Sodium	11.909	1.080	Rubidium Acid Phthalate
Aluminum	8.337	1.559	Ammonium Dihydrogen Phosphate
Silicon	7.126	1.838	Ammonium Dihydrogen Phosphate
Chromium	2.291	5.998	Lithium Fluoride
Nickel	1.659	8.337	Lithium Fluoride

(c) Determination of Mass Absorption Coefficients: In order to assess the magnitude of the interaction of the emitted x-rays with the materials comprising the sample, the mass absorption coefficients[8] were listed for the x-ray lines chosen for analysis. These data are shown in Table III.

TABLE III

MASS ABSORPTION COEFFICIENTS

EMITTER $K_{\alpha 1,2}$	ABSORBER O	Na	Al	Si	Cr	Ni
O	*	*	*	*	*	*
Na	4109	0	1021	1332	7943	12806
Al	1503	3359	386	503	3000	4838
Si	966	2168	3493	328	1955	3152
Cr	39	91	149	183	88	142
Ni	16	37	61	75	310	59

Values for μ/ρ in cm^2/gm
*No data available

With the completion of these preliminary steps, the EBM was used for the specific analyses described in Section III.

2. Scanning Electron Microscopy

An adjunct technique to electron beam microanalysis is scanning electron microscopy. As explained previously, most EBM systems can detect and display the secondary electron response from a sample under bombardment with a beam of high energy primary electrons. The resultant scanning electron micrographs yield structural information about the surface of the device.

Since an EBM was designed primarily for chemical analysis, the electron optics were chosen to provide beam currents sufficiently high enough to generate a statistically significant number of characteristic x-rays. At the same time, beam diameters on the order of a few thousand angstroms were considered optimally small.

A scanning electron microscope (SEM), on the other hand, was designed along similar lines, but the major emphasis was placed on beam diameters of approximately a few hundred angstroms. The resultant decrease in the beam current was of no consequence since these instruments were intended to provide only high resolution structural information.

The SEM used on this study was manufactured by the K^2 Corporation. The 150 angstrom beam diameter of this instrument provided the necessary spatial resolution of the scanning electron micrographs for the study of defects in the deposited glass films on the test devices. This structural information, when combined with the x-ray spectrochemical data obtained with the EBM, was used to develop a more comprehensive understanding of the factors responsible for the observed electrochemical reaction.

3. Mass Spectrometry Methods

Although the two electron beam techniques were the principal analytical methods used for this investigation, mass spectrometry was also performed on the ambient gas within the hermetically sealed devices. The two major aspects of this study were:

(a) Package Hermeticity Evaluation* Using a Veeco Helium Spectrometer Leak Detector, the leak rates of the hermetic packages were measured after exposure to helium gas under high pressure. This technique was used

*Hermeticity is a term denoting the ability of a package to prevent exchange of its internal gas with the external atmosphere. A figure of merit associated with this property is the gaseous leak rate of the package measured in atm-cc/sec.

to determine whether the moisture present inside the package resulted either from a loss of hermeticity or from its introduction during device processing.

(b) Residual Gas Analysis: An independent study was performed with a quadrupole mass spectrometer system specially modified to analyze the constituents of the package ambient. This technique determined the amount of water vapor in the package. These results are included to help explain the results obtained with the electron beam methods.

III EXPERIMENTS AND RESULTS

The following set of experiments was performed to explain the influence of the various factors present in a completed integrated circuit on the failure of these devices under low temperature biased operation.

A. OPTICAL CHARACTERIZATION OF FAILED Ni-Cr RESISTORS

The first step in this program was a definition of the general nature of the reaction in question. Devices which failed electrical testing at temperatures as low as -10 C were examined on a metallograph after removal of the package lid. Figure 5 shows several regions on this device which had undergone an attack of the Ni-Cr resistor elements. The two major features of the Ni-Cr attack were:

(1) Reaction of the thin film resistor near the edge of the aluminum interconnection stripes. This reaction normally takes place in a rather large region (A) extending under the deposited glass layer a distance of a few mils from the interface region.

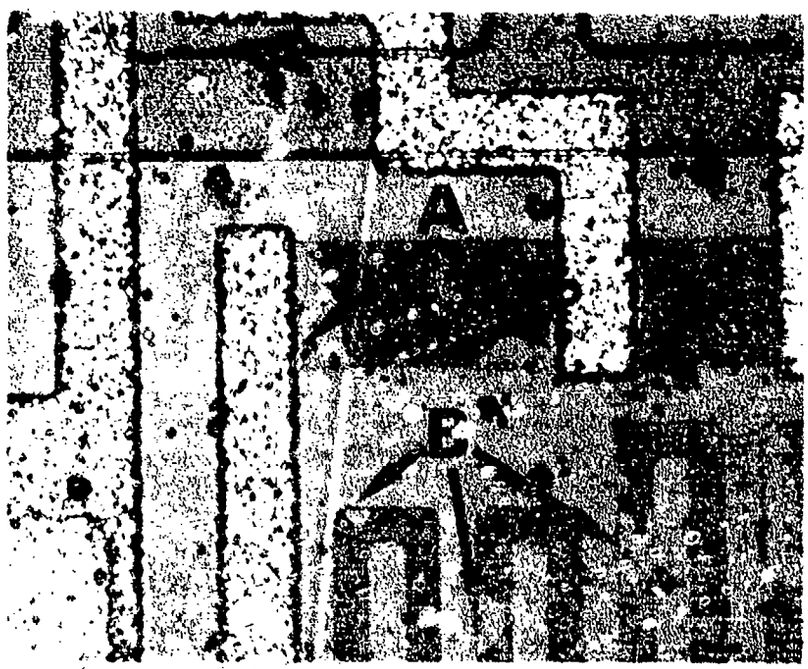

Figure 5. Failed Ni-Cr Resistor Elements

(2) Isolated reaction, indicated by the removal of the resistor-material in a circular region (B) located principally at the edges of the resistor element. The severity of this reaction varied from device to device, but the general characteristics were always identical.

B. EBM CHEMICAL CHARACTERIZATION

Before performing any detailed analysis of the corroded Ni-Cr resistors, a complete characterization of the chemical constituents of both the package and of the active chip was made.

By scanning the full complement of crystal spectrometers of the EBM over the entire x-ray spectral range, the major constituents of the various package parts were qualitatively analyzed. A list of the detected elements is given in Table IV. In general, these results were typical of one class of the all-ceramic packages used by the microelectronics industry. The interesting part of this analysis was the detection of significantly high concentrations of sodium in both the lead frame and lid seal glasses. The presence of this alkali metal atom will be shown to have a significant effect on the failure of the Ni-Cr films.

TABLE IV

CERAMIC PACKAGE CHEMICAL CONSTITUENTS

PACKAGE PART	ELEMENTS PRESENT
Ceramic Body	Aluminum Magnesium Oxygen
Lid Seal Glass	Lead Zinc Sodium Silicon Oxygen
Lead Frame Glass	Sodium Magnesium Aluminum Silicon Oxygen

In addition to the information about the package chemistry, EBM analyses of the surface of the integrated circuit indicated that the deposited glass layer was pure SiO_2, i.e., not doped with phosphorous or boron as is done in some instances, and that the thin film resistors contained more chromium than nickel. Based on the ratio of the x-ray intensities for these elements, the film composition is approximately 60 Cr: 40 Ni. This result alone is interesting since normally Ni-rich evaporation sources are used. The reasons for the change in film stoichiometry have been previously explained in terms of the increased vapor pressure and greater sticking coefficient of Cr when simultaneously evaporated with Ni from a single filament source[9].

In addition to finding a similar 60 Cr: 40 Ni film composition, Bicknell, et al, also determined, using electron diffraction, the presence of two phases in the condensed films. Approximately 60% of the Cr in the film was in a separate phase which had a structure similar to δ-Fe(OOH) and contained appreciable amounts of oxygen. All of the Ni was found in another phase having a composition of 70 Ni: 30 Cr. This phase was distributed in the form of small islands throughout the larger Cr phase. The only effect of temperature on these films was to increase the grain size of the Ni-rich phase without appreciably altering the Cr-rich matrix.

Since the test films on this program are assumed to have a similar structure, these findings will be used to explain their behavior when subjected to electrochemical attack.

C. SEM STRUCTURAL CHARACTERIZATION

After optical examination of failed Ni-Cr resistor films, it was apparent that the glassivation layer deposited over both the aluminum and thin film resistors was not like the ideal layer shown in Figure 1. From the location of the various reacted regions, one could surmise that in the SiO_2 overlay there were large defects which provided a path for moisture and other contaminants to the Ni-Cr material.

To gain a more complete understanding of the nature of the glass layer defects, several samples of both stressed and unstressed devices were examined with the scanning electron microscope. Initially, all devices were coated with a few hundred angstroms of evaporated gold to enhance the contrast of the scanning electron micrographs.

Figure 6 shows, in the deposited glass layer, one type of defect (A) which extends along the edge of an aluminum metallization stripe. The line (B) running perpendicular to this defect is due to the edge of the Ni-Cr resistor. Because the geometry of the top and bottom edges of the SiO_2 layer match, the inference is that the aluminum stripe edge was covered with a continuous layer of glass during its deposition. At a later time a crack developed due to either large intrinsic tensile stresses in the glass or differential expansion between the aluminum metallization and SiO_2 during subsequent high temperature processing. Although there are several possible manufacturing procedures during which this could happen, the most likely one is the lid sealing operation, requiring temperatures in excess of 450° C for several minutes. A recent study[10] of the thermal effects on deposited glass films encountered during integrated circuit processing discusses these problems in considerable detail.

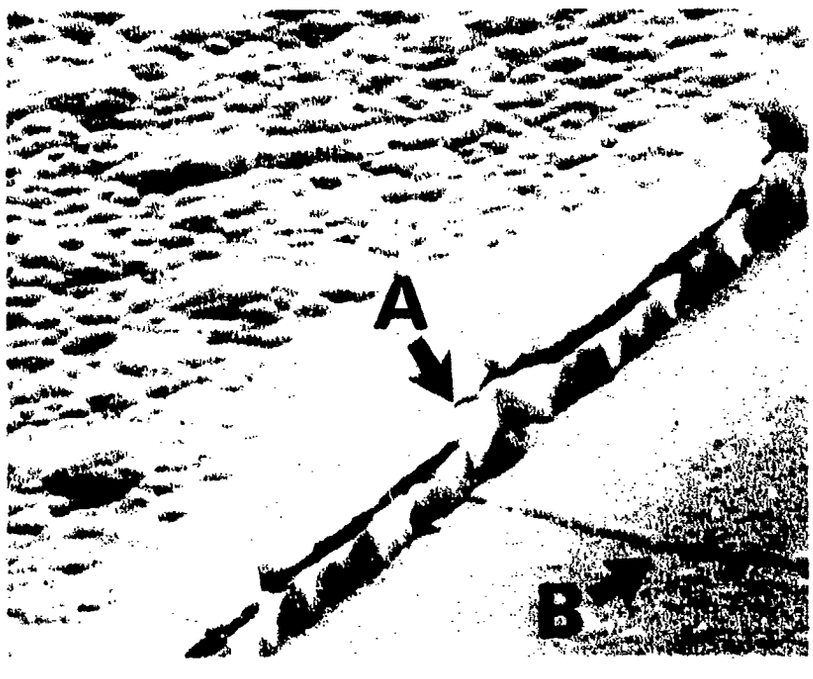

Figure 6. SEM Micrograph of Crack in Deposited Glass Layer (6,600 X)

In contrast to the type of crack shown in Figure 6, Figure 7 is a micrograph of a defect which was an artifact of the glass deposition technique. The greater width of this crack implies that the edge of the aluminum stripe was never completely covered with glass. This situation often occurs when there are geometrical design problems in the vacuum deposition equipment.

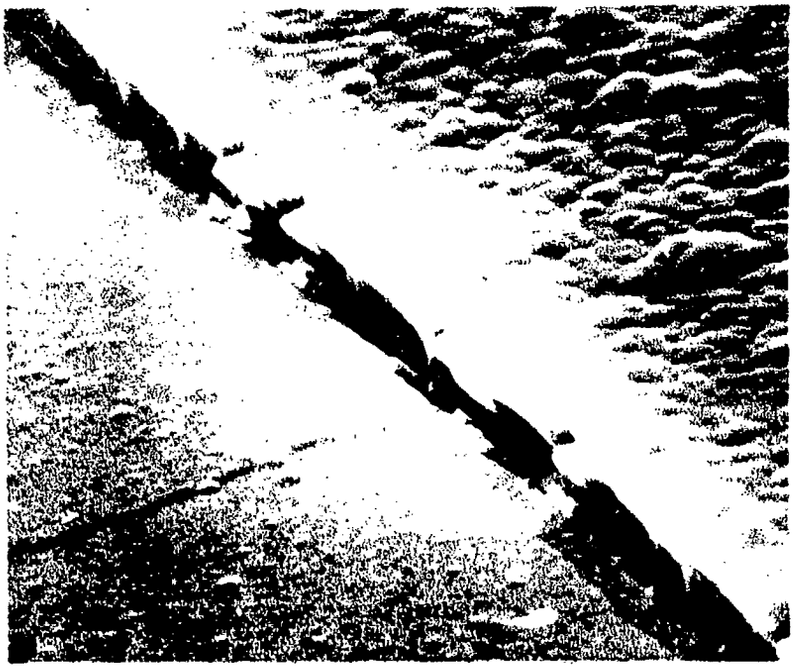

Figure 7. SEM Micrograph of Gap in Deposited Glass Layer (6,600 X)

The small pinhole-type defects (Figure 5, area B) along the edges of NiCr resistors are more difficult to explain. They may arise from an anomalous nucleation and growth of the deposited glass at these points. A study[10] of a similar phenomenon was performed on the growth of vacuum deposited aluminum films at steps in thermally grown SiO_2 on silicon.

Finally, all devices examined with the SEM had cracked glass layers such as shown in Figures 6 and 7. The cracks were found in both stressed and unstressed circuits.

IV. EBMS STUDIES OF DECAPPED DEVICES

The first test used to establish the basic aspects of the attack of the NiCr films was to observe the behavior of a device with a drop of water placed on its surface. Although the test was not very controllable, it did establish the necessity of applied potential in causing thin film resistor failure. Circuits, without any potential applied to the resistors, operated properly even after 24 hours of immersion in water.

In the first devices analyzed with the EBM, resistor failures were generated by the Thermospot Cold Probe. In this test, decapped devices were subjected to temperature cycling between room temperature and -30°C with voltage applied. The low temperature portion of the cycle was used to condense moisture from the lab ambient atmosphere which then accelerated the resistor attack at the higher temperatures.

Figure 8 shows a typical thin film Ni-Cr resistor (R) which failed after undergoing the thermospot test.

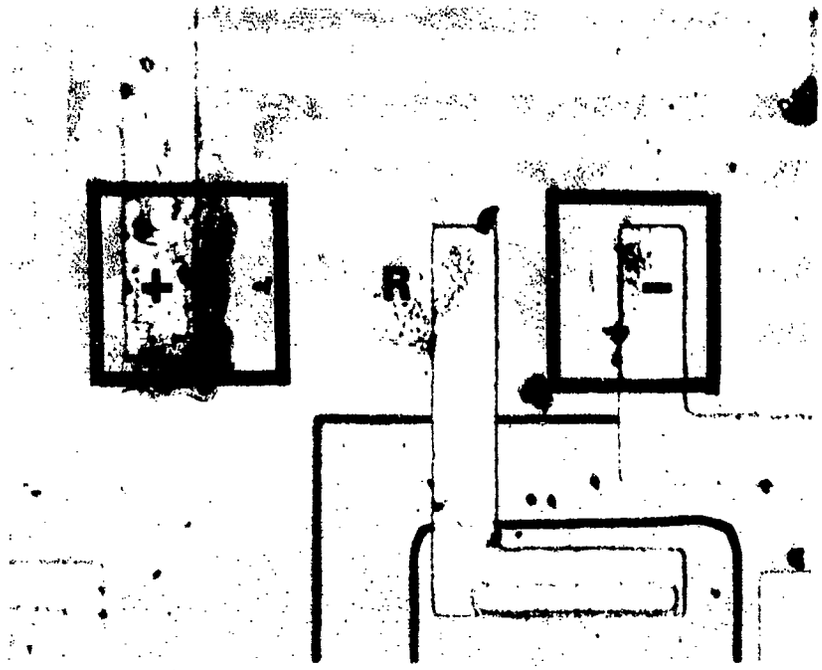

Figure 8. Failed Cold Probe Test Film

The polarity at each end of the resistor stripe is indicated. In order to determine qualitatively the distribution of the various constituents in these areas, scanning x-ray micrographs were taken for aluminum, silicon, nickel, and chromium. The results of the analysis of the rectangular area at the positive end of the resistor are presented in Figures 9a through 9d.

The most important features of these micrographs are:

(a) The slight reduction of both Cr and Ni in the resistor area.

(b) The build-up of Ni and, to a lesser degree, Cr around the edge of the aluminum stripe.

The results of similar analyses of the negative end of this resistor are shown in Figure 10. Although there is a depletion of Ni and Cr in the resistor stripe, there is no build-up of these elements near the edge of the aluminum conductor.

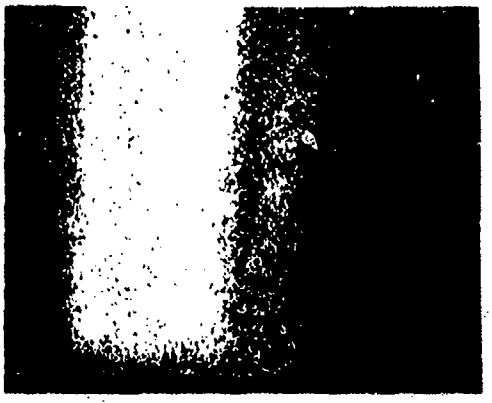

Aluminum K-Alpha
(a)

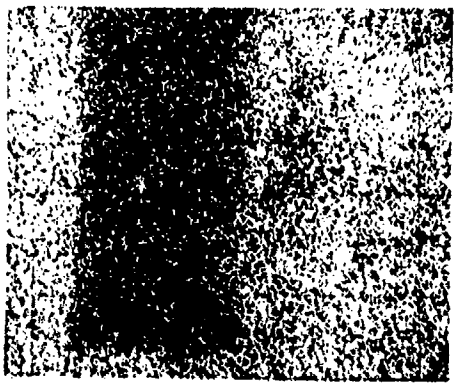

Silicon K-Alpha
(b)

25 Kilovolts

10 μm

Nickel K-Alpha
(c)

Chromium K-Alpha
(d)

Figure 9. Scanning X-Ray Micrographs-Positive Contact of Cold Probe Failure

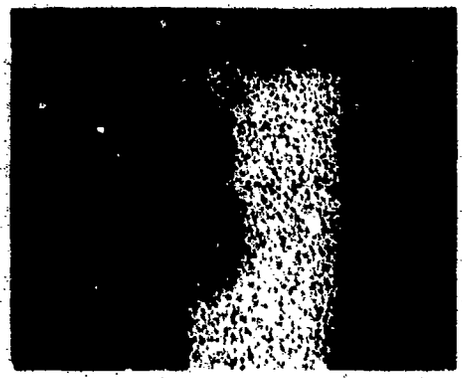

Aluminum K-Alpha
(a)

Silicon K-Alpha
(b)

25 Kilovolts
10 μm

Nickel K-Alpha
(c)

Chromium K-Alpha
(d)

Figure 10. Scanning X-Ray Micrographs-Negative Contact of Cold Probe Failure

Investigation of other resistor stripes on this device confirmed the tendency for high Cr and Ni x-ray intensities only at the edge of positively biased aluminum conductors. This same reaction was observed on all devices which underwent this particular test.

It was apparent from the x-ray micrographs of failed films that the reaction involved the formation and transport of a negative complex ion of Cr and Ni since there was no indication of cation transport to negative contacts. The next conclusion was that the material deposited at the anode should be salt-like or insulating compounds of Ni and Cr rather than the free metals. This fact was verified by the observation of visible light emitted from the larger precipitates when struck with the primary electron beam. This phenomenon, called cathodoluminescence, occurs only in materials which have a sufficiently large band gap such that direct interband transitions, excited by the high energy electrons, result in the emission of an optical photon.

Because of the rather large quantities of reactant products available on these failed films, it was easy to perform EBM qualitative analyses for the anions present in the Ni and Cr compounds. A complete spectral scan was performed on various failed devices. The only element detected, in addition to Ni and Cr, was oxygen. Since it was difficult to distinguish the exact stoichiometry of the compounds, they were assumed to be either hydrated oxides or hydroxides of chromium and nickel formed from the transport of negative hydroxyl complexes of these elements to the anode of an electrolytic cell. Further evidence in support of this assumption will be presented in Section IV.

E. EBM STUDIES OF HERMETIC DEVICES

Once the general characteristics of Ni-Cr films attacked in the known presence of water were established, the next set of experiments was performed to explain their behavior in hermetically encapsulated devices. Prior to conducting a variety of low temperature tests designed to enhance moisture condensation and accelerated thin film corrosion, the hermeticity of all test devices was evaluated using a Veeco MS-9 leak detector. The various packages exhibited leak rates in the range of 2 to 4 x 10^{-8} atm-cc/sec.[12]. These rates are below the arbitrarily determined limit of 1 x 10^{-7} atm-cc/sec defined for a well sealed hermetic ceramic package. The hermeticity test was designed to eliminate any device with a large package defect which would allow water penetration other than by diffusion through the bulk glass or ceramic materials. Although these initial leak rates were acceptable, there was, as will be shown later, some indication that moisture was being driven into the package during some of the various stress tests.

Tests were conducted on approximately 100 of the hermetic circuits and nearly 10% failed due to the electrochemical attack of the Ni-Cr resistors. A photograph of one such failed resistor is shown in Figure 11. While the voiding (V) in the resistor (R) near the edge of the aluminum contact was similar to the results of the cold probe test, generally the attack was less severe. This might be expected when only small amounts of water are available.

The EBM chemical analysis of the positive resistor contact, indicated by the rectangular area of Figure 11, resulted in the scanning x-ray micrographs shown in Figure 12. These photos are almost identical to the results of Figure 9, showing a depletion of both nickel and chromium in the resistor stripe and the build-up of the x-ray intensities of these elements near the edge of the aluminum. X-ray scans of the negative contact area of this resistor showed removal of the resistor materials but no edge build-up.

After chemically characterizing over 30 such failed regions on hermetic devices and comparing the results with initial observations on circuits which underwent attack on the water drop and thermospot tests, it was evident that a single mechanism was involved in all cases, i.e., the electrochemical attack of the Ni-Cr films in the presence of a condensed ionic medium.

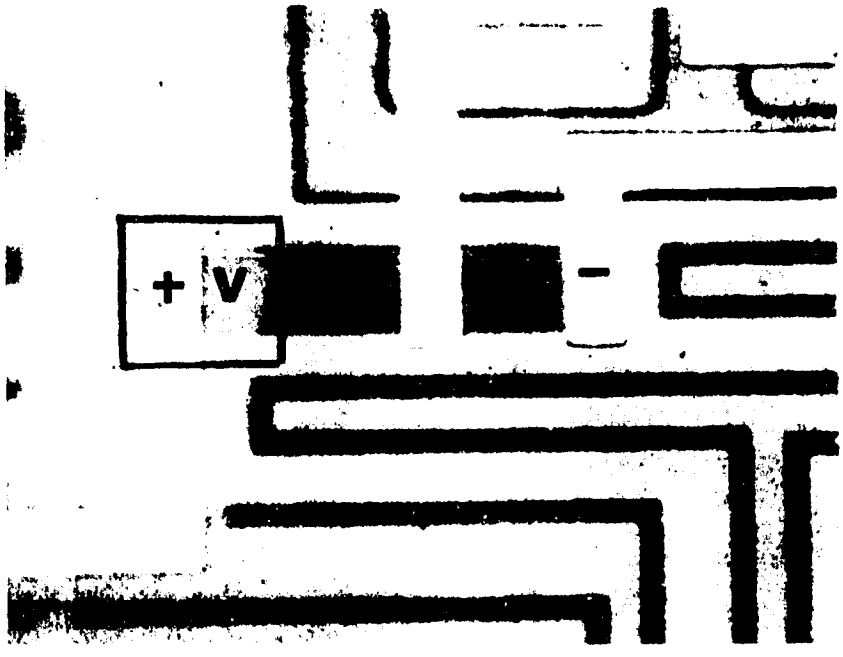

Figure 11. Failed Hermetically Encapsulated Test Film

F. RESIDUAL GAS ANALYSIS OF AMBIENT GAS IN HERMETIC PACKAGES

Although results of the low temperature testing program indicated that water vapor present inside the package cavity of hermetic devices was the most likely cause of the Ni-Cr film failures, a more quantitative evaluation of this possibility was necessary. The difficult task of analyzing the internal package gas was accomplished with a quadrupole mass spectrometer system designed with a special package puncturing fixture. A hermetic device package was first pumped down to the ultimate pressure attainable with the bakeable, ion pumped system. After the background peaks for the mass peaks of interest were taken, the ceramic lid was fractured and the mass spectrum recorded for the 10^{-2} cm^3 volume of gas within the package.

Table V is a summary of the residual gas analysis for water vapor within devices which underwent various stress conditions.[13] As can be seen from these data, failed circuits had over twice as much water vapor present than in the nonfailed stressed units. Also, devices which were analyzed immediately after they were received had the lowest concentration of moisture in the package. In addition to definitely establishing the presence of H_2O inside failed hermetic devices, this analysis also indicated that the stress tests might be effective in causing an increase in its concentration. A detailed evaluation of the various package properties which could cause this effect is much too broad for discussion at this time.

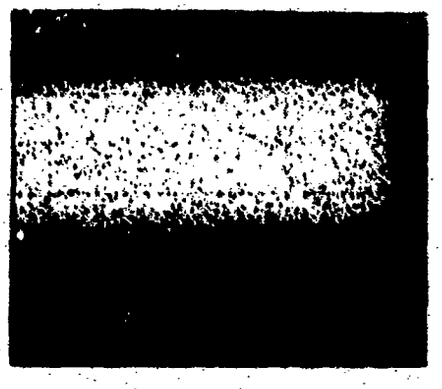

Aluminum K-Alpha
(a)

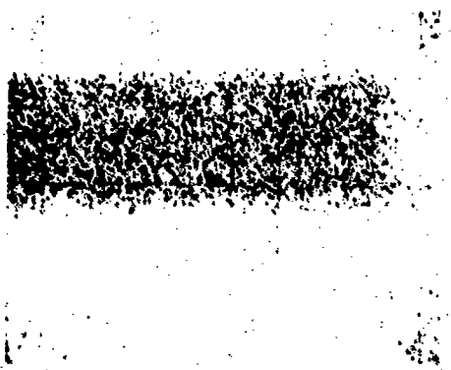

Silicon K-Alpha
(b)

25 Kilovolts
10 μm

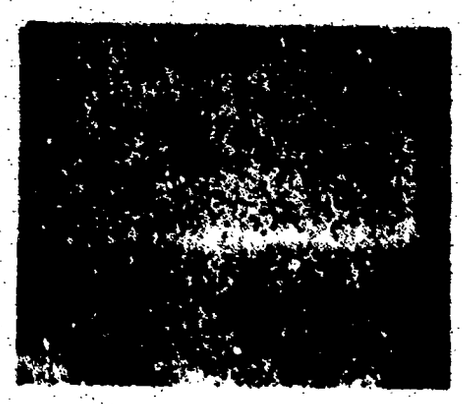

Nickel K-Alpha
(c)

Chromium K-Alpha
(d)

Figure 12. Scanning X-Ray Micrographs-Positive Contact of Hermetic Failure

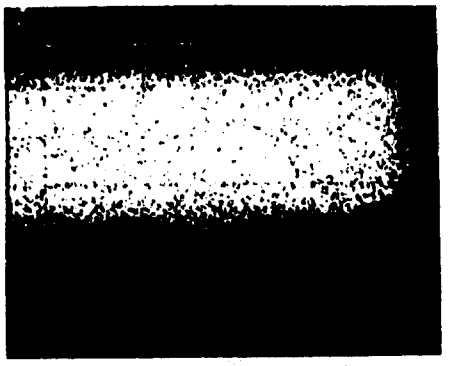

Aluminum K-Alpha
(a)

Silicon K-Alpha
(b)

25 Kilovolts
10 μm

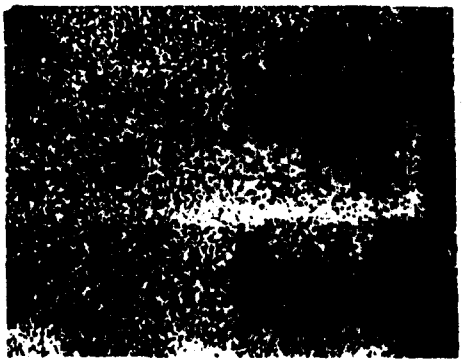

Nickel K-Alpha
(c)

Chromium K-Alpha
(d)

Figure 12. Scanning X-Ray Micrographs-Positive Contact of Hermetic Failure

TABLE V

PACKAGE AMBIENT MOISTURE ANALYSIS

DEVICE CONDITION	PERCENT WATER VAPOR
Failed Circuits	1.68
Stressed Circuits (Non-Failures)	0.72
New Circuits	0.32

G. TRACE CONTAMINATION ANALYSIS USING THE EBM

At this point in the investigation, the analytical results indicated that water vapor, condensed at low temperature, could attack the biased Ni-Cr resistors via defects in the deposited glass film. The principal chemical reaction involved the reaction of both nickel and chromium in the presence of excess hydroxyl ions.

There were several difficulties in explaining our results:

(1) Although all failed devices had sufficient water vapor present to cause corrosion, there were significant variations in the testing time required to cause failure. These variations didn't correlate with the moisture content inside the package, i.e., some devices which had a certain percentage of water vapor lasted much longer than devices which had only half that percentage.

(2) It was originally hypothesized that the excess hydroxyl ion concentration needed for the Ni-Cr attack resulted only from the electrolysis of condensed water. This hypothesis was seriously questioned in light of this failing when the applied potential was much less than the hydrogen overpotential at either an aluminum or nickel-chromium contact. Although this value of potential was never experimentally checked, literature reviews indicated that it was on the order of 1 volt. Ni-Cr resistors which failed at less than a few tenths of a volt potential required a mechanism other than electrolysis. A possible answer was the ionization of water by a chemical impurity such as an alkali metal.

The original chemical characterization of the device package indicated significantly large concentrations of sodium in both the lid and lead frame sealing glasses. Since this element forms a strong base in aqueous solution, an EBM search was undertaken to establish its presence on the surface of the integrated circuits.

To optimize the sensitivity of the chemical analysis, an accelerating potential based on the electron range calculations shown in Table I was chosen. Voltages between 15 and 25 kilovolts assured proper penetration of the electrons through the deposited and thermally grown oxide layers and yet resulted in the smallest volume of analyzed material compatible with proper x-ray line peak-to-background values for the Na K-α line.

After searching various points on the device surface, there were indications that a significantly high level of Na x-ray intensity was observable within cracked regions in the deposited glass. Nevertheless, the signal level was too low to permit taking scanning x-ray micrographs for this element.

A stationary electron beam was positioned alternately on an edge region near the cracked glass and at another point away from these areas. The output of the light element detector, using a rubidium acid phthalate crystal, was integrated on a ratemeter and used to drive a strip chart recorder. Figure 13 is one such recording taken from a failed device.

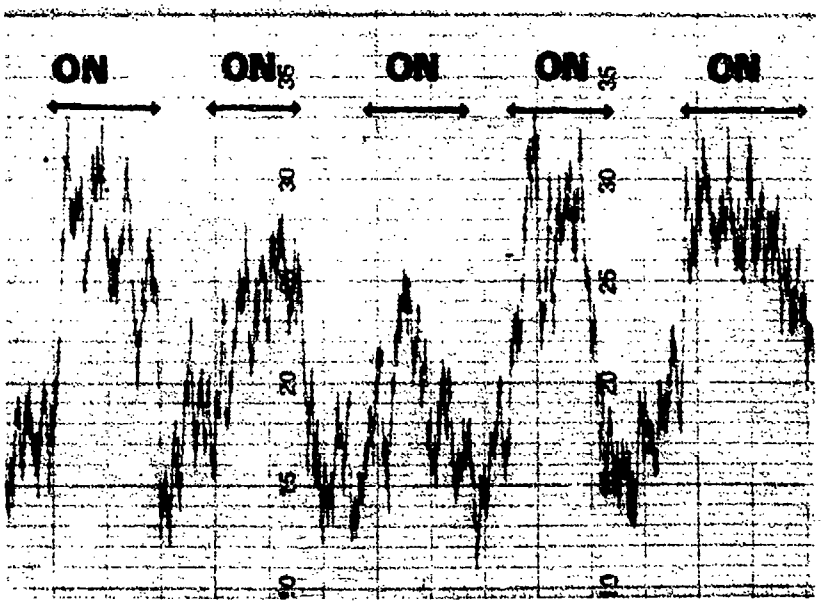

Figure 13. Sodium K-Alpha X-Ray Intensity Variation on Failed Ni-Cr Film

The response in the chart regions indicated by the word "ON" is the sodium x-ray intensity from several different edges of aluminum stripes. The response between the alternating "ON" regions is the sodium signal from arbitrarily chosen points on flat surfaces of the glass layer. This low level signal is essentially the background reading for the sodium K-alpha line.

The variation in the x-ray intensity is significantly large and shows a definite build-up of sodium near the exposed edges of aluminum metallization stripes. An analysis of similar regions of the circuit with a defocused x-ray spectrometer indicated that this intensity variation did not arise from geometrical effects due to scattering of the electron beam or other such artifacts.

The general results of the EBM analysis of 19 devices, both good and failed, are shown in Table VI. The arbitrary intensity levels were established based on the observed peak-to-background ratio of the sodium line: HIGH = greater than 2-to-1; MED = less than 2-to-1; and LOW = no significant variation in x-ray intensity, or a peak-to-background of 1-to-1. Care was taken to keep the analysis conditions identical in order to make valid comparisons of the relative intensity variations observed not only on a single circuit but from one device to another.

A closer examination of the production date codes of all these devices indicated that the low concentration of sodium occurred for two lots of circuits and that ones with the highest sodium count rates were from one particular lot. This "lot dependence" will be further discussed in Section IV.

TABLE VI

SODIUM CONCENTRATION ANALYSIS

DEVICE NUMBER	LOT NUMBER	CIRCUIT CONDITION	Na CONCENTRATION
V - 1	A	N	LOW
V - 2	A	N	MED
V - 3	A	N	HIGH
Z-4	A	F	HIGH
Z-7	A	F	HIGH
A - 5	A	F	MED
A - 10	A	F	HIGH
A - 6	A	SNF	MED
A - 36	A	SNF	HIGH
Z - 5	A	SNF	MED
G - 1	A	SNF	LOW
G - 2	A	SNF	LOW
G - 3	A	SNF	LOW
B - 1	B	N	LOW
B - 2	B	N	LOW
B - 3	B	N	LOW
C - 1	C	N	MED
C - 2	C	N	LOW
C - 3	C	N	LOW

CODE: N = NEW F = FAILURE SNF = STRESSED NON-FAILURE

H. CORRELATION OF SODIUM CONTAMINATION LEVEL AND THE RATE OF NICKEL-CHROMIUM RESISTOR ATTACK

Once the EBM was found to be effective in determining variations in the concentration of sodium at defect sites in the deposited glass layer, an experiment was performed to try to explain differences in the time-to-failure of devices stressed under identical test conditions.

Two failed devices which had been analyzed with the mass spectrometer system to determine the amount of water vapor present within their packages were chosen for this part of the study. Device number A-5 had a 3% water vapor content. The other circuit, A-10, had about 1.4%. These relative values for moisture content did not correlate with the fact that A-10 survived only two hours of testing whereas A-5 didn't fail until after 19 hours.

The sodium x-ray intensity variations at defect sites on the two failed circuits are shown in Figure 14. Device A-10 exhibits a greater sodium concentration than device A-5. These data suggest a direct relationship between the amount of sodium near the Ni-Cr film and the rate of the electrochemical attack. Further evidence supporting these findings has been established using ion beam microanalysis techniques.[14] Circuits with high concentrations of sodium and potassium in glass defect sites also were attacked most rapidly in the presence of water and applied potential.

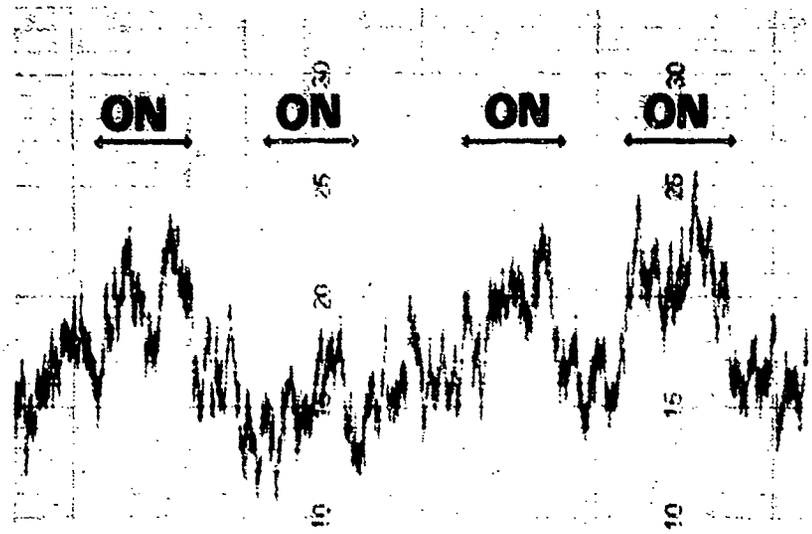

(a)
A-5

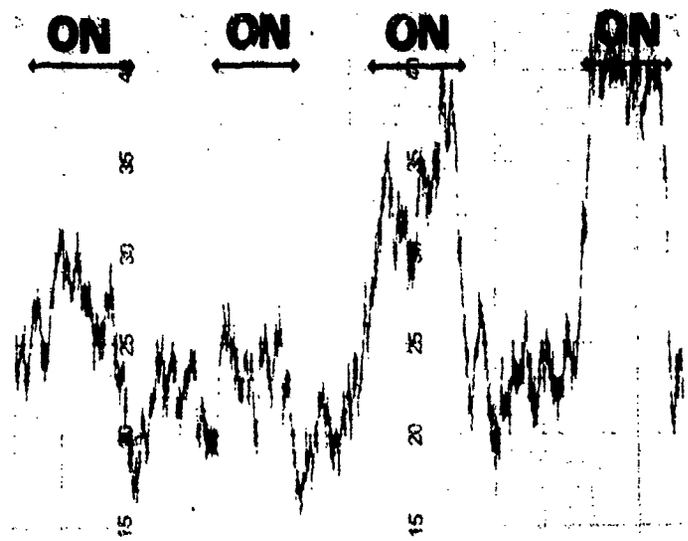

(b)
A-10

Figure 14. Sodium K-Alpha X-Ray Intensity Variation from Device Number A-5 and A-10

IV. DISCUSSION OF RESULTS

The various experiments which have just been discussed indicated that four factors were responsible for the electrochemical corrosion of Ni-Cr films:

(a) Moisture present inside the device package.

(b) Defects in the protective glass layer which allowed moisture to react with the Ni-Cr resistors.

(c) Applied potential which resulted in the transport of negative complexes of nickel and chromium to anode contacts.

(d) Sodium contamination which appeared to accelerate the reaction.

These observations will now be combined with known chemical and physical phenomena to form a model for the attack of Ni-Cr films as found on our test circuits. To accomplish this task, let us consider the first two of the above factors and their interrelationship.

A. EFFECTS OF MOISTURE AND GLASS LAYER DEFECTS

Several corroborating experiments indicated that moisture was necessary to cause Ni-Cr film failure. The results of electrical and environmental stress testing also showed temperature cycling rather than a steady-state temperature condition to be more effective in generating Ni-Cr film failures. An explanation of this behavior was developed from a consideration of the process which is most likely responsible for moisture condensation in the cracks and pinholes in the deposited glass film. The dominant mechanism appears to be capillary condensation.

This well known phenomenon of preferential condensation of moisture in fine pore structures was described by Zsigmondy[15] in terms of the equilibrium vapor pressure depression which takes place above a curved liquid surface. As explained in a more recent text,[16] vapors which are at partial pressures less than the normal saturation value are preferentially absorbed or condensed in cracks and pores which have concave surfaces. In addition to explaining preferential condensation in glass defect sites at temperatures higher than the "dew point" value for a flat surface, this mechanism also requires a much higher pressure for desorption over the surface of the liquid than is needed for absorption. Simply stated, once a crack becomes wet, it tends to stay wet.

Within the framework of this mechanism, our test sequence can be explained as follows:

(a) The temperature is lowered to a point where capillary condensation can take place. Water is then trapped within the microscopic defects in the glass film.

(b) Once water is condensed, any increase in the temperature will not cause an equivalent desorption. Thus, at the higher portion of the temperature cycle, the major effect was the acceleration of the chemical reaction which caused the removal of Ni and Cr from biased resistor films. Continued operation at the top of the temperature cycle would eventually result in desorption, necessitating the return to the low temperature level where preferential absorption would again provide the moisture needed to sustain the electrochemical attack.

Our test results substantiated this sequence of events. Continuous monitoring of the integrity of the Ni-Cr resistors during the temperature cycling experiments indicated that nearly all of the films failed during the rising temperature portion of the cycle. There was apparently some trade-off between the amount of absorbed water and the rate of chemical reaction within a given range of temperatures. This combination of the proper amount of water

at a suitably high temperature resulted in the optimum condition for resistor attack. We also found an increase in the reaction rate under cycled rather than steady-state bias conditions. This test arrangement was chosen to minimize device temperature rises due to joule heating of the resistor films since these higher temperatures would aid in the water desorption process.

There is one final note on the deleterious effects of the various types of defects in the glassivation layer of these circuits. Early use of Ni-Cr films for hybrid circuit applications indicated no problem due to the corrosion of the thin film resistors. Because this type of device didn't require the higher package sealing temperatures used on our test circuits, no deposited glass layers were needed to prevent film oxidation.

This interesting result tends to imply that no passivation layer is better than a faulty continuous passivation layer. This should be expected if one considers that: (1) preferential condensation will not take place, and (2) a more uniform electrode process will govern the corrosion of the smooth surface of the uncoated resistor.

This latter point of electrode processes has received recent attention in a thesis by Shuck.[17] A detailed analysis of the transport equations which govern chemical corrosion at cracked and pitted regions of an electrode indicated that variations in the electrolyte composition in these areas could lead to an increased rate of attack.

B. ELECTROCHEMICAL REACTION MODEL

The last ask in the analysis of the failure of the thin film Ni-Cr resistors was to combine the concept of preferential condensation at glass defect sites with the chemical information obtained with the electron beam microanalyzer. The remaining two factors which will be considered are:

(a) The build-up of nickel and chromium compounds at the most positively biased resistor contact; and,

(b) The presence of sodium contamination on the surface of the test devices.

The major difficulty in performing the chemical analysis was the minuscule amounts of materials involved in the reaction. Assuming bulk density values for both nickel and chromium, the average amount of resistor material removed from any given resistor was on the order of a nanogram. Judiciously choosing the EBM accelerating potentials used for the analysis provided for the proper determination of the major reactant products. Therefore, the qualitative wavelength searches with the various crystal spectrometers were sufficiently sensitive in establishing the absence of all elements other than nickel, chromium, oxygen, and sodium in the reacted films.

In addition to the difficulty in performing an exact analysis for oxygen due to the presence of the glass layer over the resistor films, the major substrate interference with the emitted x-rays was experienced during the sodium analysis. The mass absorption coefficients, shown in Table III, reflect this fact. In addition, there is little absorption of the nickel and chromium K-alpha x-rays in passing through the deposited glass film. An exact value of the mass absorption coefficients for the various x-rays in glass could not be calculated due to the lack of suitable data for the oxygen K-alpha line. Nevertheless, the general conclusions of analyzing the various factors affecting x-ray production and detection indicate that the intensity variations presented in both the scanning x-ray micrographs and the strip chart recordings represent true variations in the concentrations of the different elements in the analyzed regions.

With assurance that the chemical behavior of the films was as accurately determined as possible with the EBM, an investigation of known chemical reactions was undertaken in order to explain the observations.

There are two possible reactions when nickel and chromium are exposed to aqueous solutions.[18] Either the complex cations:

$Ni(H_2O)_6^{++}$ and $Cr(OH)_6^{++}$ are formed, or when excess hydroxyl ions are present,

$Ni(OH)_3^-$ and $Cr(OH)_4^-$.

The presence of sodium on the surface of the device would cause ionization of water to take place and provide the excess OH^- concentration. This fact, coupled with the build-up of material at anode contacts, implies that the Ni-Cr resistors are failing as the result of the formation and transport of the metal-hydroxyl anions.

The rate at which material reaches the positive electrodes is determined by Faraday's Law of Electrolysis. As the negative ions undergo electron exchange at the anode, compounds such as: $NiO \cdot xH_2O$ and $Cr_2O_3 \cdot xH_2O$ can be formed. There are other possibilities such as nickel hydroxide and other oxides of chromium. The first compounds have the properties of being insoluble in both water and sodium hydroxide solutions. This fact could explain the stability of the observed reactant products in the presence of these solutions within the cracks in the glass. Although sample geometry and chemistry precluded an exact determination of the reactant products, the qualitative analyses tend to confirm the presence of either oxide or hydroxide compounds of both nickel and chromium.

The amount of water needed to cause these types of reactions is on the order of a few nanograms. Recalling the data presented in Table V, the average amount of water observed in a hermetic device package would correspond to an absolute amount of water in the microgram range. This calculation indicates that there is more than enough water to cause the reaction in sealed devices.

A little better understanding of the microscopic processes which take place at the Ni-Cr electrode can be gained by a closer examination of the scanning x-ray micrographs shown in Figure 12. As may be noted, there is a higher concentration of the nickel rather than the chromium compound near the edge of the positively biased aluminum conductor. It is also evident that the nickel is preferentially removed from the reacted resistor film. This effect is so pronounced that in some cases a resistor will still have electrical continuity, even though there is little detectable nickel present in the reacted regions. In light of the EBM characterization of the test films and their similarity to those described in Reference 9, there is reason to suspect the preferential attack of the Ni-Cr metal phase of the resistor. The Cr phase would be attacked much slower because it already exists in a partially oxidized state.

There are other possible explanations for the enhanced reaction of nickel, but they would require the selective corrosion of nickel in the presence of metallic chromium. This concept is quite hard to reconcile with the fact that nickel is less reactive than chromium. The idea of a partially oxidized layer of chromium that is more impervious to attack than an unoxidized Ni-Cr phase would be in better agreement with the EBM data.

The last point to consider is the necessity for an electrochemical rather than a simple chemical reaction to cause failure. As explained earlier, very little is known about the behavior of electrolytes in fine cracks and capillaries. One can only postulate that in the absence of an applied potential, the reaction of the hydroxyl ions with the Ni-Cr film results in electrode polarization processes similar to those encountered in standard electrochemical cells.[19] These processes may prevent further chemical attack until the complex nickel and chromium hydroxyl ions are transported to an anodic contact. During this ionic transport, an unreacted surface of the resistor could be exposed to further hydroxyl ion attack. A more definitive explanation of this point could be reached only by special electrochemical studies designed to determine the important parameters such as the degree of electrode polarization and transport numbers for the nickel and chromium complex ions. This elaboration, needless to say, was not considered within the scope of this investigation.

C. DEVICE PROCESSING CONSIDERATIONS

As stated in the introduction to this report one of the most serious limitations encountered when thin film resistor elements are incorporated on an active monolithic integrated circuit is the difficulty in achieving compatibility between the thin film materials and the rest of the standard device processing steps and materials.

The complementary analytical techniques used on this program have helped to establish the major problems observed in one class of devices and the interrelationship of the various structural and chemical factors.

Integrated circuit processing, especially the deposition of the protective glass overlay, has a very important influence on the performance of the Ni-Cr resistors. All devices in this study had poorly fabricated glass films. The presence of severe defects in the glass made all devices susceptible to moisture penetration and attack. Even if an ideally perfect SiO_2 layer could have been deposited, it would still have to withstand the subsequent device processing steps. The most critical of these procedures, as inferred from the structural and chemical analyses performed on this study, is the final lid sealing operation.

In addition to the thermal stresses introduced during the high temperature sealing operation, there is the added possibility of the outgassing of impurities from the various parts of the package. This outgassing may likely be the source of the sodium contamination. The addition of this element to the glass parts of the package may appear rather imprudent in light of the observed chemical reactions with the Ni-Cr films. The major reason for the use of sodium and other alkali metals is to modify the thermal expansion properties of the different glasses. This is essential in order to assure a proper seal between the dissimilar package parts and is especially critical for a durable glass-to-metal seal at the device lead frame.

During the course of this study, a paper[20] was published on the various problems associated with device packaging. As Deal states in this work, two of the critical areas associated with the glasses used in ceramic packages were:

(a) The outgassing of chemical impurities during sealing.

(b) The attack of the device metallization by moisture.

Although sodium was specifically isolated by Deal as a contributor to device failure, the major point of concern was its influence on the silicon surface properties. His discussion applies equally well to our test devices provided the weakest point of the integrated circuit is the vulnerability of the Ni-Cr resistors to chemical attack rather than the susceptibility of the device to failure from surface-related effects.

The dependence of the severity of the effects of sodium contamination on device processing may be inferred from Table VI. The strong lot dependence for high sodium concentration suggests the loss of control on either processing or the quality of the materials used in the device package. There are so many operations during which the package is prepared for final seal that it is conceivable that one of them resulted in the excess sodium outgassing on lot A and not on the others. The types of manufacturing procedures which could lead to these results could not be determined by any chemical analysis techniques with the EBM. This type of a study could be effectively performed only by the device manufacturer or package supplier. Only they would have the visibility into the specific processing steps.

There is another interesting fact about the influence of sodium on device failure that is shown in Table VI. There are three stressed non-failed devices, i.e., A-6, A-36, Z-5, which have significant levels of sodium contamination within defect regions in the glass layer. These devices were removed from the stress tests after a specified period of time. These devices may not have failed due to a lack of sufficient moisture to sustain the electrochemical attack. Some water vapor must have been present since it is believed that the sodium reacts with the Ni-Cr films by the action

of water leaching this element from contaminated surfaces within the device package and its subsequent preferential condensation in the glass defect sites. This interpretation is in agreement with the results of the internal package gas analysis. Water was found in all packages but only devices with a level of about 1.7% failed.

This brings us to the last critical area associated with device production. Although cracked glassivation and sodium contamination are important contributors to the Ni-Cr resistor attack, moisture is the necessary factor. Therefore, one must assure an initially dry package and one which maintains its hermetic seal integrity over the entire temperature range anticipated for device use.

We normally assume that any moisture that is present within the device enters after final sealing operation. This assumption was unfounded in this study since new devices had nearly 0.2% water vapor content in the internal package gas. This may have resulted from sealing in a wet atmosphere or from outgassing of the package during lid seal. As tests were performed on these circuits, the water vapor level increased. This can be attributed to a loss of hermeticity of the package. The insidious point about this problem is the limitation on our methods for determining gaseous leak rates for ceramic packages. The results of this study were inconclusive in determining any loss of hermeticity. Each device exhibited a gaseous leak rate which was "in the noise" both before and after the stress tests.

V SUMMARY AND CONCLUSIONS

The electrochemical attack of thin film Ni-Cr resistors is contingent on the presence of the following factors

(1) The availability of moisture within the cavity of the hermetic device package.

(2) Biased operation of the test devices at temperatures at which moisture can condense on the device surface.

(3) A defective glass layer over the thin film resistors.

(4) The presence of sodium contamination on the surface of the integrated circuit.

These results were obtained using the electron beam microanalyzer and scanning electron microscope in conjunction with mass spectrographic gas analysis techniques. Within the limitations of the chemical analysis methods afforded by the EBM, the reactant products of failed resistor films were identified as oxide or hydroxide compounds of nickel and chromium.

These observations were evaluated in light of known physical and chemical phenomena which could be operative in the presence of the four critical factors. The major reactions were:

(1) The preferential condensation of water in cracks and pinholes in the deposited glass layer.

(2) Hydroxyl ion attack of nickel and chromium, accelerated by the ionization of water by sodium.

(3) The electrochemical transport of negative hydroxyl ion complexes of nickel and chromium and the subsequent build-up of compounds of these materials at anodic contacts.

Within the context of the proposed model for the attack of the thin film resistors, several recommendations are offered as a means of minimizing the susceptibility of monolithic integrated circuits to this problem:

(1) The use of a defect-free deposited glass. This may necessitate the use of other deposition techniques such as the pyrolysis of silane gas, or composite methods such as vacuum deposited SiO_2 followed by silane SiO_2. These processes would promote better coverage of the edges of the aluminum conductor stripes, thereby eliminating the large gap type of defects observed on our test devices. There still might be pinholes with these types of glasses, and these pinholes could lead to failure if located near a Ni-Cr film. Care must be exercised that any glass used for a protective overlay be capable of withstanding the thermal stresses imposed by such operations as device lid sealing.

(2) The elimination of contaminants within the device package. The major reactant which must be controlled is water. Secondly, elements such as sodium or other chemical accelerators must also be eliminated. These procedures require a three-fold approach.

(a) Eliminate any source of moisture within the atmosphere inside the sealing furnaces. This standard requirement for all types of semiconductor devices can be difficult to accomplish. Even though circuits without Ni-Cr resistors are less susceptible to small variations in package moisture content, the use of 150 Angstrom films imposes the need for more stringent controls in this area.

(b) Reduce the amount of contaminants which can outgas from the package materials both before final lid seal and during subsequent high temperature device operation. In order to accomplish this task, improved pre-sealing package treatment processes are needed. The major area for control lies in the methods used to handle

the lid sealing glass. This material is applied to the ceramic lid in the form of a slurry. This slurry is then fired to form a solid at a temperature below the glass devitrification temperature encountered during lid seal. Improper outgassing of this material during the pre-firing operation can lead to the injection of moisture into the package during the final sealing operation.

Along these same lines, the elemental constituents of the glass package parts may themselves outgas during the high temperature sealing operation. The presence of sodium on the device surface has been attributed to this process. The elimination of this accelerating factor for film corrosion can be accomplished by not using this element as a glass modifier. On the other hand, this could lead to poor thermal expansion properties of the glass and the failure of the hermetic seal. Another alternative is the use of a lower temperature sealing process. Although some available solder glass-ceramics seal at a lower temperature than that used on these devices, the variation is only slight and would not appreciably minimize the outgassing of elements such as sodium which have high vapor pressures at those temperatures.

(c) Assure package hermetic seal integrity over the entire temperature range anticipated for device use. The sealing process requires the compatibility of all materials used in the device package. Other than the porosity of the ceramic material itself, the most critical areas in causing loss of hermeticity are the glass-to-metal lead frame seals and the package lid seal. Difficulties in achieving this goal using ceramic packages may necessitate a change to a completely different system such as an all-metal package.

In conclusion, the results of this study have led to a more comprehensive understanding of the interaction of many of the chemical and physical factors which lead to the electrochemical attack of thin film Ni-Cr resistors. Because the integrated circuits studied on this program were typical of other microcircuits using thin film resistors, the recommendations which have been outlined should provide guidelines for improved reliability of a wide variety of similar devices.

BIBLIOGRAPHY

1. Watts, R. K., "High Resistivity Thin Film Resistors for Monolithic Circuits – A Review," Solid State Technology, Vol. 12, No. 6, June 1969, pp. 64-68

2. Philofsky, E., Stickney, G., Ravi, K. V., "Observations on the Reliability of Thin Film Nichrome Resistors," Proc. 8th Reliability Physics Symposium, April 1970, pp. 191-199

3. Castaing, R., Thesis, University of Paris, 1955

4. Birks, L., Electron Probe Microanalysis, Interscience, 1963

5. Marton, L., Tousimis, A., Electron Probe Microanalysis, Academic Press, New York, 1969

6. Archard, G. D., Mulvey, T., Proc. of the Third International Symposium on X-Ray Optics and X-Ray Microanalysis, Academic Press, New York, 1964, p. 329 ff

7. Nelms, A. T., Nat. Bur. Stds. Circular No. 577 (1956) and Supplement (1958)

8. Heinrich, K. F. J., "X-Ray Absorption Uncertainty," Proc. of the Electron Microanalysis Symposium, Electrochemical Society, Washington, D.C., October 1964

9. Bicknell, R. W., Blackburn, H., Campbell, D. S., "The Structure of Vacuum Condensed Ni-Cr Films," Microanalysis and Reliability, 3, 1964, pp. 61-64

10. Ghate, P. B., "Failure Mechanism Studies on Multilevel Metallization Systems for LSI," RADC-TR-71-186, September 1971, pp. 25-42

11. Yanagawa, T., Takekoshi, T., IEEE Trans. on Electron Devices, Vol. ED-17, No. 11, 1970, p. 964

12. Hommel, B. H., Private Communication, Rome, New York, November 1971

13. Thomas, R. W., Private Communication, Rome, New York, December 1971

14. Riggs, E., Private Communication, Crane, Indiana, March 1972

15. Zsigmondy, R. Z., Z. Anorg. Chem., 71, 1911, p. 355

16. Taylor, H. S., Glasstone, S., Treatise on Physical Chemistry, D. Van Nostrand, New York, 1952, pp. 607-610

17. Shuck, R., "Corrosion and Transport Processes in Cracks," Thesis, Carnegie-Mellon University, Metals Research Lab., Pittsburgh, Pennsylvania, May 1971

18. Quagliano, J. V., Chemistry, Prentice-Hall, Englewood Cliffs, New Jersey, 1958, p. 703 ff

19. Condon, E. U., Odishaw, H., Handbook of Physics, McGraw-Hill, New York, 1958, Chapter 9

20. Deal, B. E., "Current Concepts in the Passivation and Encapsulation of Semiconductor Devices," Proc. 10th Electrical Insulation Conference, September 1971, pp. 63-68